Cryogenics 52 (2012) 609–614

Contents lists available at SciVerse ScienceDirect

Cryogenics

journal homepage: www.elsevier.com/locate/cryogenics

Enthalpy change measurements of a mixed refrigerant in a microcryogenic cooler in steady and pulsating flow regimes ☆

R.J. Lewis [a,*], Y.-D. Wang [a], M.-H. Lin [a], M.L. Huber [b], R. Radebaugh [b], Y.C. Lee [a]

[a] Center for Integrated Micro/Nano Transducers (iMINT), University of Colorado, Boulder, CO 80309, USA
[b] Thermophysical Properties Division, National Institute of Standards and Technology (NIST), Boulder, CO 80305, USA

ARTICLE INFO

Article history:
Received 1 March 2012
Received in revised form 31 July 2012
Accepted 7 August 2012
Available online 29 August 2012

Keywords:
Mixed refrigerant
Joule–Thomson
Microcryogenic cooler
Enthalpy measurement
Annular flow

ABSTRACT

Microcryogenic coolers (MCCs) are useful to a number of small electronic devices which require low cooling power. The cooling power of microcryogenic coolers operating with mixed refrigerants in a Joule–Thomson (J–T) cycle can be calculated based on enthalpy change for the mixture, but it has been observed that cooling power depends on flow regime. This article demonstrates a method to measure the isothermal enthalpy change in a mixture undergoing J–T expansion in an MCC for different flow regimes. The enthalpy change for a mixture undergoing steady flow is an order of magnitude below that calculated, whereas the enthalpy change for the mixture undergoing pulsating flow agrees with the calculations below a certain temperature, and is over-predicted above that temperature. For steady flow, an analysis of component separation within the mixture due to annular flow shows good agreement with measured data, and for pulsating flow, the discrepancy is likely due to periods of liquid slug flow interrupted by periods of annular flow.

1. Introduction

Many electronic devices benefit from operation at cryogenic temperatures. At low temperatures, such devices can have lower thermal noise and higher bandwidth, and some can attain a superconducting state. Many small electronic devices require only a small amount of cooling power, which makes microcryogenic coolers (MCCs) attractive because they can produce the required cooling power while being smaller and less expensive than the macro-scale counterparts. Previous Joule–Thomson (J–T) MCCs have used pure refrigerants, requiring high driving pressures [1–3]. Mixed refrigerants can use very low driving pressures. Several mixtures use driving pressures near 2.0 MPa [4], and recent results have used mixtures with as little as 0.4 MPa driving pressure, enabling the use of miniature scale compressors, and the prospects of micro-compressors [5].

However, an issue arises with mixed refrigerants in that the composition can change along the cooler [6], resulting in a different cooling power than expected. It has also been noted that MCCs initially experience slow cooling with steady refrigerant flow, followed by fast cooling with unsteady refrigerant flow [7]. The cooling power available with a mixed refrigerant is given as the product of the molar flow rate and the specific isothermal enthalpy change of the refrigerant as it expands from high pressure to low pressure. This article presents a method to measure the isothermal enthalpy change of a mixed refrigerant in a MCC as a function of temperature. Such measurement shows that the cooling power for an unsteady flow regime is an order of magnitude more than that for a steady regime. This low cooling power with steady flow can be understood in terms of liquid holdup in an annular flow regime.

2. Methods and materials

The ideal cooling power ($\dot{Q}$) of a J–T cryogenic cooler can be calculated as the product of the flow rate ($\dot{n}$) with the minimum isothermal enthalpy difference between the high- and low-pressure refrigerant, over the temperature range experienced by the cooler [8]: $\dot{Q} = \dot{n}(\Delta h|_T)_{min}$. Enthalpy can be calculated as a function of pressure, temperature, and refrigerant composition from an equation of state model, and the isothermal enthalpy changes can be subsequently found. The refrigerant studied in this article is a mixture composed of methane (8%), ethane (46%), propane (14%), butane (4%) and pentane (28%) (values given in molar percent). The compositions were chosen to maximize $(\Delta h|_T)_{min}$ between a high pressure of 0.4 MPa and a low pressure of 0.1 MPa, over the temperature range of 200–300 K. Although the refrigerant is designed to cool from 300 K, pre-cooling to 275 K was found to be necessary for effective cooling with MCCs using this refrigerant [5,7]. In this test, the microcooler is studied under an isothermal

☆ Partial contribution of NIST, not subject to copyright in the US.

* Corresponding author. Tel.: +1 509 438 3587.
E-mail address: rjlewis@colorado.edu (R.J. Lewis).

0011-2275/$ - see front matter © 2012 Elsevier Ltd. All rights reserved.
http://dx.doi.org/10.1016/j.cryogenics.2012.08.006

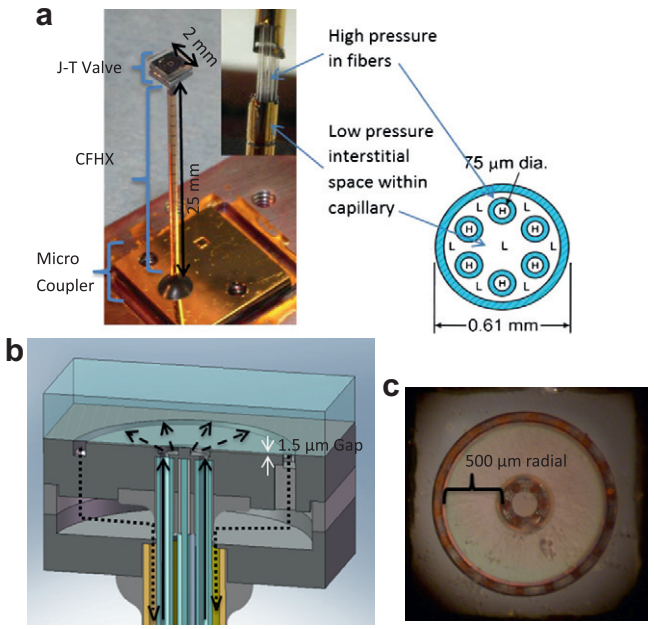

Fig. 1. The microcryogenic cooler used in this experiment: (a) photograph of the MCC, with insert showing fiber microchannels held within a capillary forming the CFHX; (b) schematic of J–T valve, showing the path of the high-pressure refrigerant (solid line) as it expands across the J–T valve (dashed line), and returns at a low-pressure (dotted line); and (c) top-view photograph of the J–T valve.

condition, where the cold-end of the MCC is actively heated until it is the same temperature as the warm-end. When there is only a single temperature experienced by the cooler, rather than a temperature range, the cooling power is given by $\dot{n}(\Delta h)$, with the enthalpy calculated at the device temperature.

The J–T MCC used in this experiment is shown in Fig. 1, and is composed of a micro-machined J–T valve, hollow-core fiber-based counter-flow heat exchanger (CFHX), and micro-coupler. Fabrication and assembly of this device are detailed elsewhere [9], but briefly covered here. The J–T valve is formed by anodic-bonding a borosilicate glass chip to an etched silicon chip. A gap between the two chips measuring 1.5 μm in height and 500 μm radially provides a flow restriction where the refrigerant undergoes Joule–Thomson expansion and cooling. High-pressure refrigerant is delivered to the J–T valve through hollow-core glass fibers with inner diameter and outer diameter (ID/OD) of 75/125 μm. The fibers are held in a glass capillary ID/OD = 536/617 μm, and the low-pressure refrigerant travels through the interstitial space between the fibers within the capillary, forming a CFHX. However, in this test the temperature across the entire cooler is ideally held at a single temperature, so no heat needs to be transferred between the low-pressure and high-pressure microchannels. Still, when the cooler acts in a non-steady flow regime, the presence of a heat exchanger allows us to quickly resolve changes in the cooling power.

The micro-coupler interfaces the MCC with the external test set-up, shown in Fig. 2. The refrigerant was compressed by a customized non-lubricated miniature compressor, described in [7]. Pressures and flow-rates of the refrigerant were monitored. It has been noted that MCCs can suffer from clogging due to ice formation from trace water in the system [10]. Previous studies with this MCC have used activated carbon adsorption systems to remove trace water [9]; however such a dryer system would also selectively adsorb some of the hydrocarbon refrigerants and change the composition of our refrigerant. Therefore, a 0.3 nm molecular sieve was used to remove trace moisture contaminants without changing the composition of the refrigerant mixture. After the molecular sieve, the refrigerant passes through a particulates filter with a

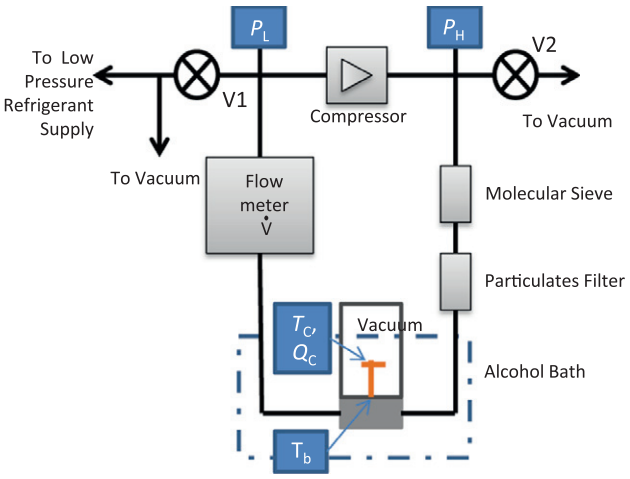

Fig. 2. Schematic of the test set-up used. Measured values include low-side pressure (P_L), high-side pressure (P_H), base temperature (T_b), cold-tip temperature (T_c), heat applied to cold-tip (Q_c), and flow-rate ($\dot{V}$). During the tests, valve 1 remains open to the low pressure refrigerant supply.

sintered mesh of 7 μm element pore size, to remove any particulate contaminants [7]. Pressure drops across the molecular sieve and filter are measured to be <0.1 kPa. Standard 1/8″ copper refrigeration tubing carries the filtered refrigerant to the MCC. The MCC was held under vacuum during the tests. The vacuum test stage and 10 cm of the coupling tubing was placed in an alcohol bath to pre-cool the refrigerant and ensure a steady yet controllable warm-end temperature. A radiation shield shrouded the MCC cold end, preventing heat loads by radiation from lab ambient conditions. The temperatures at the radiation shield, MCC base, and J–T valve on the MCC were measured with platinum resistance thermometers. A voltage was applied to the resistance thermometer at the J–T valve, which provided heating to the cold-tip of the MCC. A control loop determined the voltage to ensure that the temperature of the J–T valve was the same as that at the inlet to the CFHX, such that the device could experience an isothermal enthalpy difference.

The heat applied to the MCC by the control loop determined the net cooling power of the MCC. The gross cooling power was the sum of the net cooling power and the parasitic heat loads. Such loads are due to radiation, conduction through the DC leads, conduction through the CFHX, and conduction through the vacuum. Ideally, the entire MCC is at the same temperature as the vacuum test stage, so there would be no temperature gradients to drive conductive or radiative heat transfer. However during the test, temperature differences of up to 1 °C between the cold-tip and warm base can occur, resulting in some conductive and radiative heat loads. Radiative heat loads were calculated from the Stefan Boltzmann law with a known radiation shield temperature, known cold-tip temperature, and known MCC geometry. Conductive heat loads were calculated from a thermal resistance model, through the glass heat exchanger and DC leads with known geometry. Details of the model have been discussed in a prior publication [12]. Enthalpy change could then be calculated based on the heat load and flow-rate measurements. This measures the change in enthalpy between the high-pressure and low-pressure streams at the J–T valve. But because enthalpy is a function of temperature and pressure, and the temperature at the J–T valve is kept the same as the temperature at the warm-end inlet to the MCC, and because pressure drops in the CFHX are small be design, this will also be the enthalpy change across the entire MCC—including heat exchanger.

When the refrigerant mixture was operated at the temperature range in question, the miniature compressor could generate a high pressure of 0.337 MPa with a suction pressure of 0.100 MPa, which was open to the refrigerant supply tank, regulated at 0.100 MPa.

The tank further ensured a constant composition of the refrigerant at the compressor, which differs from the method used by Gong et al. [6], which did not use a low pressure reservoir, but rather used an initial charge in their system. The composition shift they observed was based on location in the J–T system. Our pressure in the MCC corresponds to a flow-rate that varied between 2 and 6 std. cubic cm per minute (sccm), depending on temperature. With this flow-rate over the temperature range of interest, two distinct flow patterns were observed: one with steady flow-rates, and another with pulsating flow-rates.

After data were collected for 5 min at a single temperature, the alcohol temperature was changed, the system allowed to equilibrate at the updated temperature, and data acquisition resumed. The test started with the alcohol bath at a temperature of 294 K and the MCC system operating in a steady flow regime. The bath was then cooled in increments of 2–5 K, down to 270 K. At that point the test had been operating for roughly 1 h, and the system transitioned to a pulsating flow regime. Once in the pulsating flow regime, the temperature was increased to collect pulsating flow enthalpy data in the temperature range 270–300 K. With increasing temperature, the frequency of pulsation occurrence decreased, until above 286 K the pulsations were no longer present. To get steady-flow data at lower temperatures, the lines were evacuated, re-charged with fresh refrigerant, and the test started with an alcohol bath at 270 K. After decreasing in steps to 245 K, over a period of 1 h, the system again transitioned to pulsating flow. The bath was cooled further to 240 K, below which thermal stresses began to damage seals in the coupler. The bath temperature was increased in increments in order to complete the enthalpy measurements for pulsating flow.

3. Results

The isothermal enthalpy change data for these two flow regimes are plotted against cold-tip temperature in Fig. 3. Also included is a calculation of enthalpy difference between the mixture at 0.337 MPa and 0.1 MPa as a function of temperature, as calculated by the NIST standard reference data software REFPROP [13]. Uncertainty bars come from both a variation in measured enthalpy data over the 5 min data collection time, and inaccuracies from the measurement of the parasitic loads. The parasitic loads are assumed to be accurate to 10% [12]. The statistical uncertainties are calculated from the first standard deviation in enthalpy data collected over 300 s, which includes variations in the parasitic heat loads. The parasitic loads are up to 0.3 mW, and applied heat loads are typically in the range 0.2–0.8 mW for the steady flow tests, so these loads are quite significant to the steady flow measurements. With pulsating flows, applied heat loads were in the range 5–10 mW, so statistical uncertainties were the most significant. In these cases, enthalpy data were collected over several pulsating cycles, and the standard deviation between the average enthalpy of each period of oscillation was used for the statistical uncertainty. Some of the data runs had pulses with a very regular frequency and very regular cooling power, and correspond to low statistical uncertainties; however most data runs have more erratic pulsations and cooling powers, which correspond to higher statistical uncertainties.

The transition between flow regimes represents a transition between viscosity-dominated (steady) flow and surface-tension dominated (pulsating) flow [11]. In microchannels undergoing condensation, liquid forms first as a film on the side-wall of the channel. Once the liquid is thick enough, its surface tension can overcome the viscous forces, and form liquid slugs or plugs in the channel. Our results suggest that with this refrigerant mixture at a flow-rate of 2–6 sccm, it takes roughly 1 h to reach that thickness. Furthermore, above a temperature of 286 K, the liquid fraction is too low to form liquid slugs.

4. Discussion

Note from Fig. 3 that the enthalpies measured for the pulsating flow agree well with those calculated at temperatures of 260 K and lower; however for steady flow they can be an order of magnitude below those calculated. The reason for this discrepancy lies in the liquid/vapor flow regime. With two-phase flow, the gross cooling power across a J–T valve is found from an energy balance as:

$$\dot{Q} = [\dot{n}_v h_v + \dot{n}_1 h_1]_{P_{low}} - [\dot{n}_v h_v + \dot{n}_1 h_1]_{P_{high}} = \dot{n}_{Tot} \Delta h_{FA}, \quad (1)$$

where $\dot{n}_{Tot}$ is the total molecular flow rate of both phases, the subscripts v and l refer to the vapor and liquid phases, and Δh_{FA} is the flux-averaged difference enthalpy found by re-arranging Eq. (1) to give:

$$\Delta h_{FA} = \left[\frac{\dot{n}_v}{\dot{n}_l+\dot{n}_v}h_v + \frac{\dot{n}_l}{\dot{n}_v+\dot{n}_l}h_l\right]_{P_{low}} - \left[\frac{\dot{n}_v}{\dot{n}_l+\dot{n}_v}h_v + \frac{\dot{n}_l}{\dot{n}_v+\dot{n}_l}h_l\right]_{P_{high}} \quad (2)$$

These "fluxed-averaged" quantities are the values of flow-rate and enthalpy difference measured in this test; however REFPROP calculates mixture enthalpies based on mole-averaging between phases, rather than flux-averaging.

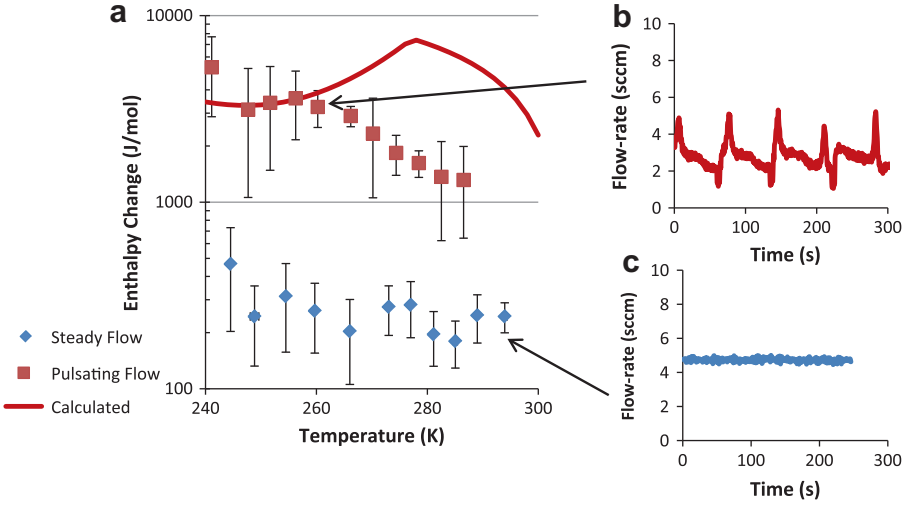

Fig. 3. (a) Measured values of isothermal enthalpy change of the refrigerant for both steady and pulsating flows as well as values calculated by REFPROP for a 2-phase mixture, plotted against cold-tip temperature. (b) Flow-rate of pulsating flow at 260 K, (c) flow-rate of steady flow at 294 K.

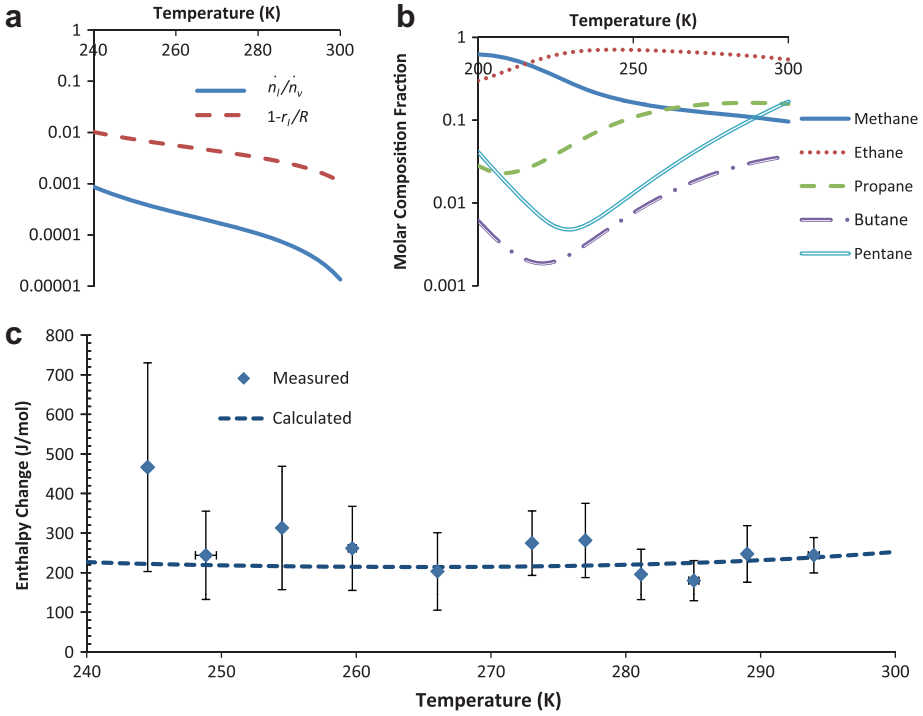

Fig. 4. (a) Ratio of molar fluxes $\frac{\dot{n}_l}{\dot{n}_v}$, and a non-dimensional thickness of the liquid film $1 - r_l/R$, over the temperature range of interest, (b) molar composition of the vapor-phase of the refrigerant when at 0.337 MPa, for various temperatures, (c) measured isothermal enthalpy change for steady flow, and Δh values calculated with Eq. (2)–(4), plotted against MCC cold-tip temperature.

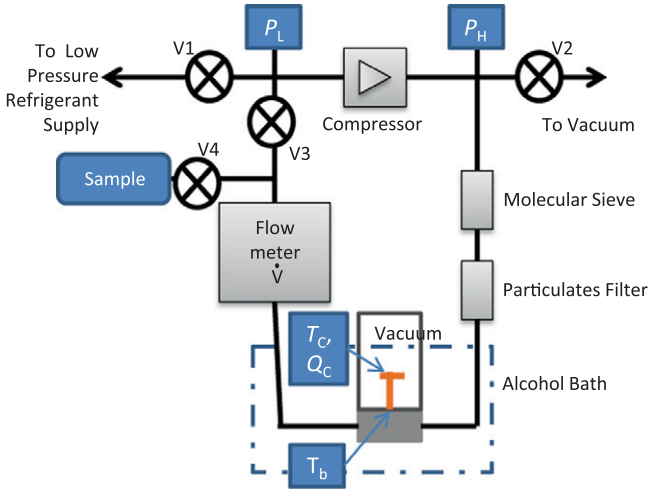

Fig. 5. Modified test set-up, to sample the refrigerant mixture that passed through the MCC.

The ratio of vapor mole flux to liquid mole flux depends on the flow regime. Initially, as the system cools, heavy components in the refrigerant condense on the sidewalls of the microchannels, and the system experiences annular flow. With low flow-rates in microchannels, the ratio of fluxes can then be calculated from Stokes theory, as [14]:

$$\frac{\dot{n}_l}{\dot{n}_v} = \frac{\rho_l}{\rho_v} \frac{-1 - \left(\frac{r_i}{R}\right)^4 + 2\left(\frac{r_i}{R}\right)^2}{-2\left(\frac{r_i}{R}\right)^4 - \left(\frac{r_i}{R}\right)^4 \frac{\mu_l}{\mu_v} + \left(\frac{r_i}{R}\right)^2} \tag{3}$$

where ρ represents molar density, μ dynamic viscosity, R the channel radius and r_i the radius to the liquid/vapor interface. In a cylindrical geometry, r_i/R can be calculated from the vapor quality (X) of the mixture and liquid and vapor densities as:

$$\frac{r_i}{R} = \sqrt{\frac{\frac{X}{\rho_v}}{\frac{X}{\rho_v} + \frac{1-X}{\rho_l}}} \tag{4}$$

Physical properties of each phase can be calculated by REFPROP. Because the density of the liquid is much more than that of the vapor, the value of r_i/R will be close to 1, and consequently $\frac{\dot{n}_l}{\dot{n}_v} \ll 1$. The values $1 - r_i/R$ and $\frac{\dot{n}_l}{\dot{n}_v}$ are plotted in Fig. 4a for this mixture with a pressure of 0.337 MPa and the temperature range 240–300 K. Note that the ratio of liquid to vapor mole-flux is $<10^{-3}$ for this mixture over the temperature and pressure range seen during steady flow. Note also from Eqs. (3) and (4) that the ratio of liquid-to-vapor flow-rates is a function of fluid properties, but not the size of the channel in question. This analysis can be applied to the coupling channels as well as the microchannels.

All components that liquefy in the high-pressure channels adhere to the walls, and only small amounts pass through the J–T valve and contribute to cooling. Liquid films are observed in the J–T valve, as shown in Fig. 6f. Because the mixture is non-azeotropic, the vapor has a different composition than that of the overall mixture, which is a function of both temperature and pressure, shown in Fig. 4b.

Operating in such a mode will cause a composition shift at the MCC, but as the compressor is open to a 160 L reservoir and we are moving refrigerant at <10 sccm, it would over 4 h to effect a 1% change in the composition of any component in the total system. Because steady flow only persists for 1 h, it is assumed that the composition shift is localized to the MCC, and the compressor provides a feed of constant composition. The dashed curve in Fig. 4c shows the flux-averaged enthalpy change of the refrigerant in annular flow, as calculated by Eq. (2) and (3), for a high pressure of 0.337 MPa at each temperature. Physical quantities are

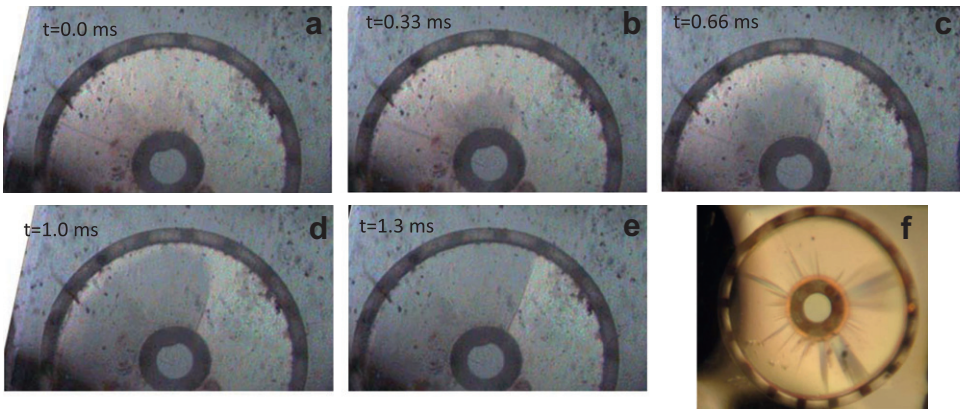

Fig. 6. (a–e) A slug of liquid passes into the J–T valve over the course of 1.3 ms, taken at a frame-rate of 3000 frames per second (fps). This slug event corresponds to a pulse in the flow-rate during pulsation flow; (f) wisps of liquid film in the J–T valve during steady flow, taken at a frame-rate of 30 fps.

Table 1
Molar percentages of refrigerant mixture collected during steady flow at 295 K, 273 K, and 250 K, determined by GC/TCD analysis. Compositions of the vapor portion of the mixture are included, as calculated by REFPROP at the temperature and pressure specified.

	295 K at 0.397 MPa		273 K at 0.375 MPa		250 K at 0.336 MPa	
	Measured	Calculated	Measured	Calculated	Measured	Calculated
Methane	10.15	10.14	11.71	12.13	13.78	15.06
Ethane	55.93	56.58	63.12	64.29	69.71	70.22
Propane	16.30	16.02	16.95	15.81	14.18	12.21
Butane	3.69	3.45	2.82	2.22	1.21	0.93
Pentane	13.82	13.81	5.37	5.55	1.11	1.58

calculated with REFPROP, showing good agreement with measured values for steady flow.

To confirm that the composition through the MCC is indeed changing, we performed a separate test to sample the refrigerant that passed through the MCC. The modified test setup is shown in Fig. 5. In this test, the refrigerant was compressed, passed through the filters and pre-cooled lines, passed through the heated MCC where it experienced isothermal expansion, and then was collected. During an initial period, valve 4 is closed and valve 3 is open, such that the system runs in a closed-cycle and allows the high pressure to build up. Once the system reaches its equilibrium high-pressure, valve 3 is closed and valve 4 is open, and the system runs in an open-cycle capacity while a 300 mL sample is collected. Three samples were taken at 295 K, 272 K, and 250 K, during steady flow. The high-pressures that the compressor was able to generate during these three tests were 0.397 MPa, 0.375 MPa, and 0.336 MPa, respectively. The collected refrigerant was analyzed with gas chromatography/thermal conductivity detection (GC/TCD), with results shown in Table 1. Also included in Table 1 are the compositions of the vapor components, calculated with REFPROP. The calculated values show generally very good agreement with the measured values.

Once the temperature is low enough and liquid fraction high enough, the surface-tension force of the liquid will overcome the inertial force of the vapor core, and the annular flow will transition into slug flow [15]. Each pulse in flow-rate corresponds to a slug of liquid, as verified by observing flow in the J–T valve, shown in Fig. 6. Although ice clogging has been observed for MCCs, it is not expected to occur at temperatures above 200 K [10], and is not seen here. One expects that if slugs occur with high enough frequency, the ratio $\dot{n}_l/(\dot{n}_{Tot})$ will be equivalent to the liquid mole fraction $(\frac{n_l}{n_{Tot}})$ and the measured Δh_{FA} value will agree with that calculated by REFPROP. However as the temperature increases and the slugs become further spaced, it is likely that each instance of slug flow will be separated by periods of annular flow, causing the enthalpy of a full period of oscillation to decrease. As a result, a MCC system running this refrigerant requires pre-cooling to <275 K in order to achieve the high cooling powers available to the two-phase flow.

5. Conclusions

The conclusions of this article are summarized as follows:

- This article demonstrates a method to measure the enthalpy difference of a mixed refrigerant in a J–T MCC.
- The measurement shows an order-of-magnitude difference between the enthalpy change of refrigerant in a steady flow regime and that of a pulsating regime.
- The measured low cooling power for steady flow agrees well with values calculated by the expansion of a mixture dominated by the vapor components of the refrigerant, as predicted by an annular flow pattern in which low flow-rates of liquid prevent the liquid components from contributing to the cooling.
- Measured values for pulsating flow agree with calculated values when the temperature is below 260 K. The deviation above 260 K is likely due to periods of annular flow separating liquid slugs. The lower-than-calculated values of isothermal enthalpy difference will decrease the $(\Delta h|_T)_{min}$ value for systems with entrance temperatures above 260 K for this mixture and MCC, accounting for the need for pre-cooling.

Acknowledgements

This work is supported by the DARPA Microcryogenic Cooler Program with Grant numbers NBCHC060052 and W31P4Q-10-1-0004.

References

[1] Little WA. Microminiature refrigeration—small is better. Physica 1982;109–110B:2001-9.
[2] Burger JF, Holland HJ, Seppenwoolde JH, Berenschot E, ter Brake HJM, Gardeniers JGE, et al. 165 K micro cryocooler operating with a sorption compressor and a micromachined cold stage. Cryocoolers 2001;11:551–60.
[3] Lerou PPPM, Venhorst GCF, Berends CF, Veenstra TT, Blom M, Burger JF, et al. Fabrication of micro cryogenic coldstage using MEMS technology. J Micromech Microeng 2006;16:1919–25.

[4] Chakraghavan VS, Shah RK, Venkatarathnam G. A review of refrigeration methods in the temperature range 4–300 K. J Therm Sci Eng Appl 2011;3:020801-1.
[5] Lewis RJ, Wang Y, Cooper J, Lin M-H, Bright VM, Lee YC, Bradley PE, Radebaugh R, Huber ML. In: Infrared technology and applications XXXVII: proceedings of the SPIE defense, security, and sensing symposium, vol. 8012, Orlando, Florida; April 2011. p. 8012–75.
[6] Gong M, Deng Z, Wu J. Composition shift of a mixed-gas Joule–Thomson refrigerator driven by an oil-free compressor. Cryocoolers 2007;14:453–8.
[7] Lewis RJ, Lin M-H, Wang Y, Cooper J, Bradley P, Radebaugh R, Huber M, Lee YC. Demonstration of a micro cryogenic cooler and miniature compressor for cooling to 200 K. In: Proceedings of the international mechanical engineering conference and exposition, Denver, Colorado; November 2011. p. 63908.
[8] Radebaugh R. Recent developments in cryocoolers. 19th International congress of refrigeration; 1995. p. 973–89.
[9] Lin M-H, Bradley PE, Wu H-J, Booth JC, Radebaugh R, Lee YC. Design, fabrication, and assembly of a hollow-core fiber-based micro cryogenic cooler. In: Solid-state sensors, actuators and microsystems conference, 2009. TRANSDUCERS 2009. International Denver, Colorado; June 2009. p. 1114–7.
[10] Lerou PPPM, ter Brake HJM, Holland HJ, Burger JF, Rogalla H. Insight into clogging of micromachined cryogenic coolers. Appl Phys Lett 2007;90:064102.
[11] Garimella S, Killion JD, Coleman JW. An experimentally validated model for two-phase pressure drop in the intermittent flow regime for circular microchannels. ASME J Fluids Eng 2002;124:205–15.
[12] Lin M-H, Bradley PE, Booth JC, Lewis RJ, Radebaugh R, Lee YC. Low power micro cryogenic cooler achieved by ultra-high thermal isolation. Presented in ASME InterPACK'11, Portland, OR; 2011. July 6–8.
[13] Lemmon EW, Huber ML, McLinden MO. NIST standard reference database 23: reference fluid thermodynamic and transport properties – REFPROP, version 9.0. National Institute of Standards and Technology, Standard Reference Data Program, Gaithersburg; 2010.
[14] See for example Equation 11 from Thierry C Tancogne S. Stability of bifluidic jets in microchannels. Eur J Mech B – Fluid 2011;30(4):406–20.
[15] Zhao JF, Hu WR. Slug to annular flow transition of microgravity two-phase flow. Int J Multiphase Flow 2000;26(8):1295–304.